

## Fluid Dynamics of a Micro-Bioreactor for Tissue Engineering

P. Yu<sup>1</sup>, T. S. Lee<sup>1</sup>, Y. Zeng<sup>1</sup> and H. T. Low<sup>2</sup>

**Abstract:** A numerical model is developed for the investigation of flow field and mass transport in a micro-bioreactor, of working volume below 5 ml, in which medium mixing is generated by a magnetic stirrer-rod rotating on the bottom. The flow-field results show that a recirculation region exists above the stirrer rod and rotates with it; the related fluid mixing is characterized by a circulation coefficient of up to 0.2 which is about five times smaller than that of a one-litre stirred-tank bioreactor. The oxygen transfer coefficient is less than  $5 \text{ h}^{-1}$  which is two orders smaller than that of a 10-litre fermentor with aeration, hence the oxygen transfer rate is insufficient for bacteria culture and bubble aeration is needed as was used in the prototype by Kostov et al. (2001). However, it is shown that for certain animal cell cultures, the oxygen concentration level in the micro-bioreactor can become adequate without using bubble aeration, provided that the magnetic rod is rotated at a high speed (rod Reynolds number of 716). At such high rotation-speed, the micro-bioreactor exhibits a peak shear-stress below  $0.5 \text{ N m}^{-2}$  that is acceptable for animal cell culture. The maximum local-energy dissipation rate is below  $18 \text{ kW m}^{-3}$  which is five times smaller than that in a ten-litre Rushton-impeller bioreactor.

**keyword:** Micro-Bioreactor, Hydrodynamic stress, Oxygen transfer, Stirred tank, Tissue Engineering.

### 1 Introduction

The in-vitro culture of mammalian cells is essential in the development of bioartificial organs and many types of bioreactor have been designed for this purpose. In bioreactor design, the fluid dynamics or transport properties are of practical importance. A basic issue is medium mixing to provide a homogeneous distribution of the substrate in order to expose all cells to optimal conditions

(Lubbert and Jorgensen, 2001). Another important issue is the mass transfer of oxygen into the medium, the rate of which is low as the dissolved oxygen-concentration for aqueous solution is low.

Over recent years computational fluid dynamics (CFD) has enjoyed an outstanding success in the investigation of bioreactor performance. There have been several computational studies on the laminar flow field and fluid mixing in large-scale industrial stirred-tank bioreactors (Harvey et al., 2000; Zalc et al, 2001). The velocity fields were computed and based on the velocities, the particle trajectories were mapped. A mixing time was then defined based on the time required for a particle to move a certain distance.

From the computed flow-field, the local shear rate at a fixed position may be obtained from the first derivatives of the velocity components. An example of such flow field and shear stress computation is given in the analysis by Begley and Kleis (2000) for the NASA rotating-wall perfused-vessel bioreactor. It was found that improved flow patterns, with better mass transport characteristics and low shear stress, may be obtained from different operating conditions, for example differential rotation speeds of inner and outer cylinders. Lappa (2003) numerically computed the velocity and shear-stress distribution around a construct in a rotating bioreactor; this analysis also considered the effect of shear stress on tissue growth rate; non-uniform tissue growth was observed on the construct, with the upstream corners having higher growth due to higher stresses.

The above literature survey indicates that many flow studies have been concerned with conventional bioreactors using large volumes of media for big-scale productions. However, large bioreactors are not suitable for conducting large numbers of simultaneous experiments to systematically study the effects of environmental parameters on cell growth. In the framework of studies devoted to the initial stages of cell culture, it is more economical and convenient to grow cells in small volumes; and multi-well culture plates have been widely used in such

<sup>1</sup> Department of Mechanical Engineering, National University of Singapore, Singapore

<sup>2</sup> Division of Bioengineering, National University of Singapore, Singapore

a context. But with such static wells, there is no medium perfusion and the mass transport is thus limited. These static wells are not suitable for high-density cell growth. To overcome this limitation, the well plates may be agitated on a rotational shaker that enhances mass transfer, thus enabling higher cell density to be cultured (Girard et al., 2001). The performance of various small scale bioreactors, with working volume below 100 ml, have been reviewed by S Kumar et al. (2004).

Kostov et al. (2001) designed a novel micro-bioreactor of working volume 2 ml that could form the basis of a multiple-bioreactor system for high throughput bioprocessing. In their novel design, a small magnetic stir bar was placed on the bottom of a 1 cm square cuvette, and the bar was magnetically rotated at 300 rpm to provide agitation. Suspended *Escherichia coli* cells were cultured in the micro-bioreactor. An optical sensing system was developed to measure the variation with time of pH, dissolved oxygen and optical density and these profiles were satisfactory as compared with those in a one-litre bioreactor. Oxygen adequacy was ensured with bubble aeration.

However, till date this novel micro-bioreactor of Kostov et al. (2001) has not been tested with other types of cells (other than suspended *Escherichia coli* cells) like mammalian cells which are less robust to fluid shear stress and more sensitive to medium mixing conditions. Furthermore it is not known whether the oxygen transfer would be adequate if the bioreactor was operated in a simpler way without the bubble aeration system. These basic fluid-dynamic and oxygen-transfer issues represent the motivation of the present study devoted to develop a computational fluid dynamics model of the flow field and mass transport in the micro-bioreactor.

In the present computational work, the flow field and oxygen concentration-field are investigated in a micro-bioreactor, consisting of a culture well in which a small magnetic stirring-rod is placed on the bottom to enhance the medium mixing. The flow and mass transport in the micro-bioreactor are studied by a numerical model based on finite-volume method. The results of velocity components, circulation coefficients, and hydrodynamic stresses are presented in non-dimensional form for general applications.

## 2 Computational Methods

### 2.1 Mathematical Model

The magnetic rod is located on the bottom and rotates about the axis of the chamber as shown in Figure 1. The chamber is filled with the medium, and does not have any microcarriers. In a typical application, the medium volume is about 4 ml. In contrast, industrial bioreactors of the stirred-tank type may be of several thousand litres in volume (Leist et al. 1990). The chamber of the present micro-bioreactor has diameter  $D$  of 22 mm and height  $H$  of 12 mm. The stirrer-rod diameter  $d$  is 1 mm and its length  $L$  is 12 mm.

The moving reference frame method is used to model the flow. In the original inertial frame, the flow is unsteady because the rod sweeps the flow domain periodically. By transferring the coordinates system from the original frame to the rotating frame of the stirrer rod, the flow is steady relative to the rotating frame. This simplifies the flow modeling. The velocities in the two reference frames are related by the following equation:

$$\vec{u}_r = \vec{u} - (\vec{\Omega} \times \vec{r}) \quad (1)$$

where  $\vec{u}$  is the absolute velocity,  $\vec{u}_r$  is the relative velocity,  $\vec{\Omega}$  is the angular velocity vector or the angular velocity of the rotating frame; and  $\vec{r}$  is the position vector in the rotating frame.

For flows in rotating domains, the equations for conservations of mass and momentum (Batchelor, 1967) may be expressed as:

$$\nabla \cdot (\rho \vec{u}_r) = 0 \quad (2)$$

$$\nabla \cdot (\rho \vec{u}_r \vec{u}_r) + \rho (\vec{\Omega} \times \vec{u}_r) = -\nabla p + \nabla \cdot (\vec{\tau}) \quad (3)$$

where  $\rho$  is the medium density,  $p$  is the static pressure, and  $\vec{\tau}$  is the stress tensor. Note that the gravitational body force and external body forces are neglected.

The substrate numerically modeled here is oxygen. Insufficient oxygen supply is one of the limiting factors in the scaling up of animal cell culture processes (Leist et al. 1990). It is envisaged that the present scaling-down process may likewise be limited by insufficient oxygen supply, especially if there is no bubble aeration. The species continuity equation is:

$$\vec{u} \cdot \nabla C = D_c \nabla^2 C - R_m \quad (4)$$

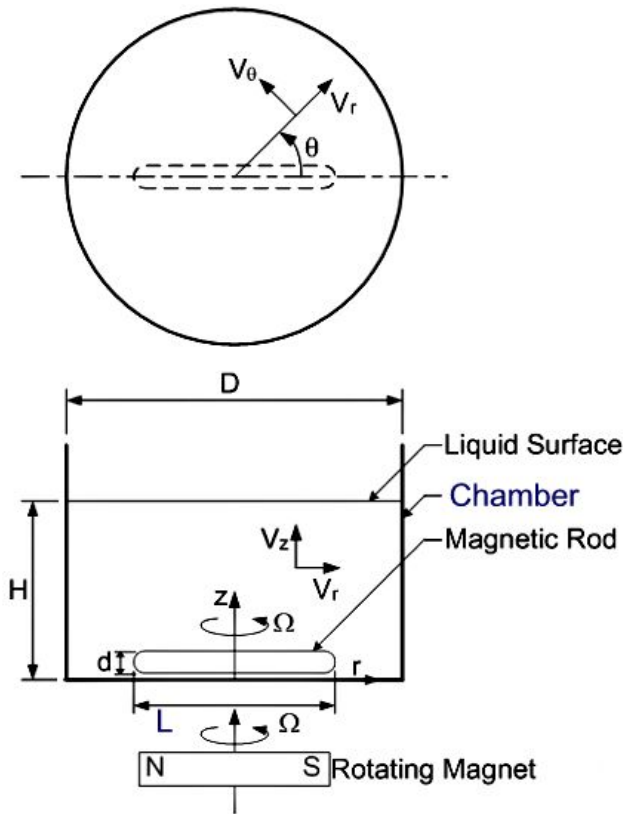


**Figure 1 :** Illustration of the micro-bioreactor system.

where  $C$  is the molar concentration ( $\text{mol m}^{-3}$ ) of oxygen,  $D_c$  is its binary diffusivity in the media ( $\text{m}^2 \text{s}^{-1}$ ) and  $R_m$  is the molar rate of species consumption per unit volume ( $\text{mol m}^{-3} \text{s}^{-1}$ ).

The oxygen consumption by the cells is based on Michaelis-Menten equation. Hence the oxygen reaction rate  $R_m$  is written as:

$$R_m = \frac{\gamma V_m C}{C + k_m} \quad (5)$$

where  $\gamma$  is the cell density in the micro-bioreactor,  $V_m$  is the maximum oxygen uptake-rate (specific) of the cell and  $k_m$  is the Michaelis constant, or oxygen concentration at which the reaction rate is half maximal. The cells are assumed uniformly suspended and their density is assumed constant throughout the process.

The no-slip conditions are imposed at the solid boundary. At the surface of the medium, the velocity is assumed

zero (Ng et al., 1999). The oxygen concentration at the surface is assumed constant and equal to the saturation concentration in the media as determined from Henry's law.

The Reynolds number based on the rod length is defined as:

$$Re = \frac{\rho N L^2}{\mu} \quad (6)$$

where  $\mu$  is the dynamic viscosity and  $N$  ( $\text{rev s}^{-1}$ ) is the rotating speed of the stirrer rod. Different Reynolds numbers from 143 to 716, corresponding to the rotation speeds from 1 to 5  $\text{rev s}^{-1}$  respectively, are simulated. Since the maximum Reynolds number is less than the critical value of 1,000 (Nagata, 1975) the flow is assumed laminar.

The non-dimensional parameter, Damkohler number, is used to quantitatively describe the nutrients consumption:

$$Da = \frac{\gamma V_m L^2}{C_0 D_c} \quad (7)$$

where  $C_0$  is the saturation concentration in the medium. As an example, a typical value of the Damkohler number can be calculated for a typical CHO cell culture from the data of Deshpande and Heinzle (2004). If the cell density  $\gamma = 1 \times 10^6 \text{ cells ml}^{-1}$ , oxygen uptake rate  $V_m = 8 \times 10^{-17} \text{ mol cell}^{-1} \text{ s}^{-1}$  and saturation concentration  $C_0 = 0.2$ , the Damkohler number is 19.6.

## 2.2 Numerical Method

The commercial software FLUENT, a finite-volume based code, was used for the numerical solution of the flow field. Commercial software such as this have been used to simulate the flow field in bioreactors by several researchers (Unger et al., 2000; Begley and Kleis, 2000; Williams et al., 2002). FLUENT uses a control-volume approach to integrate the governing equations over each cell in the mesh. The resulting set of algebraic equations are linearized and solved numerically. The second order upwind scheme was applied for discretization and the SIMPLER method was used to solve the governing equations.

It was found that in the numerical model, a small gap has to be imposed between the rod and the base of the bioreactor. Without this artifact, the commercial mesh

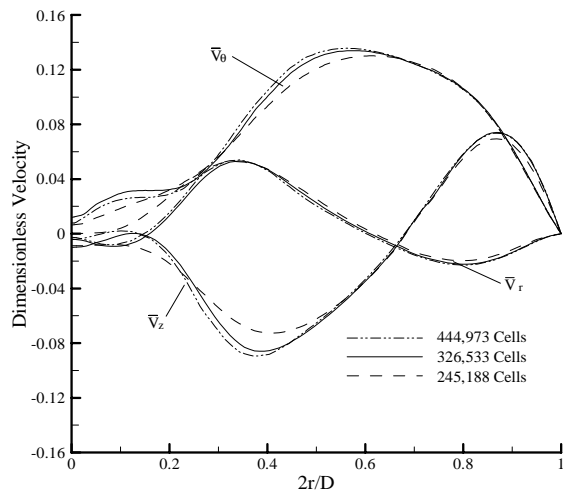


**Figure 2 :** Dimensionless velocity-components (reference =  $\pi NL$ ) versus radial position at height  $z/H = 0.125$ , Reynolds number  $Re = 716$  and angular coordinate from rod  $\theta = 90^\circ$ .

generator code GAMBIT could not generate an accurate mesh for the whole flow domain. In this study, a gap of 0.1 mm was imposed in the model.

### 2.3 Validation

For rotation flow problem, the mesh should be sufficiently refined to resolve large gradients in pressure and rotation speed. To check grid independence, a study has been performed with three sets of mesh at the highest Reynolds number of 716. The cells numbers of the three sets of mesh are 245,188, 326,533 and 444,973. Dimensionless velocity components curves for the different sets of meshes are shown in Fig. 2. As a compromise between computational accuracy and time, a mesh with 326,533 cells has been selected for the final computation.

To verify the CFD model, the flow in a tank stirred by a two-blade impeller has been simulated, using the same conditions as those in the experiments of Youcefi's (1993). The comparison of the numerical and experimental results is presented in Figure 3. The agreement indicates that the present numerical model gives velocity components with satisfactory accuracy.

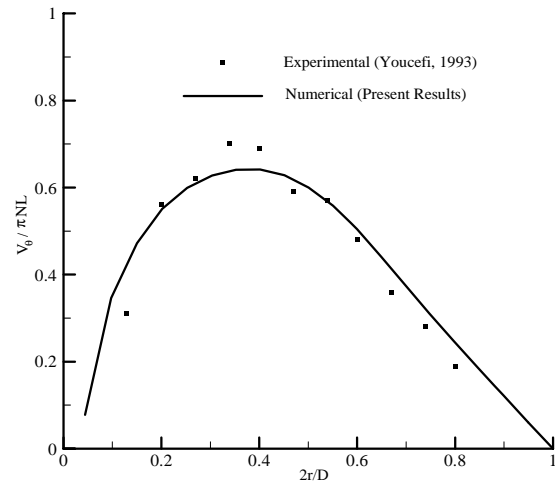


**Figure 3 :** Dimensionless tangential-velocity versus radial position at height  $z = 1.1$  mm,  $Re = 38$  and angular coordinate from impeller  $\theta = 90^\circ$ .

## 3 Results and Discussion

The results are presented for a stirring rod of length ratio  $L/D = 0.545$ , rod diameter ratio  $d/L = 0.083$  and bioreactor height ratio  $H/D = 0.545$ . The results and discussion are split into four parts: flow field, medium mixing, oxygen transfer, and hydrodynamic stress.

### 3.1 Flow Field

It is essential to know the flow field, as it indicates the extent of medium mixing in the bioreactor. The various velocity components are also needed to calculate the shear stress level and oxygen transport.

Fig 4 presents the velocity field in a vertical plane (at angle  $0^\circ$  from the magnetic rod) for three different Reynolds numbers 286, 430 and 716. It shows that the fluid in the micro-bioreactor does not behave like that of a solid body rotation which has no axial mixing. The flow pattern shows that a central recirculating-region is formed.

The fluid recoils away from the rotating rod towards the wall, where it flows upward and returns downward near the axis. This creates a recirculation flow above the stirring rod. This recirculation is weak at small  $Re$  of 286. At higher Reynolds number 430, the recirculation flow appears stronger.

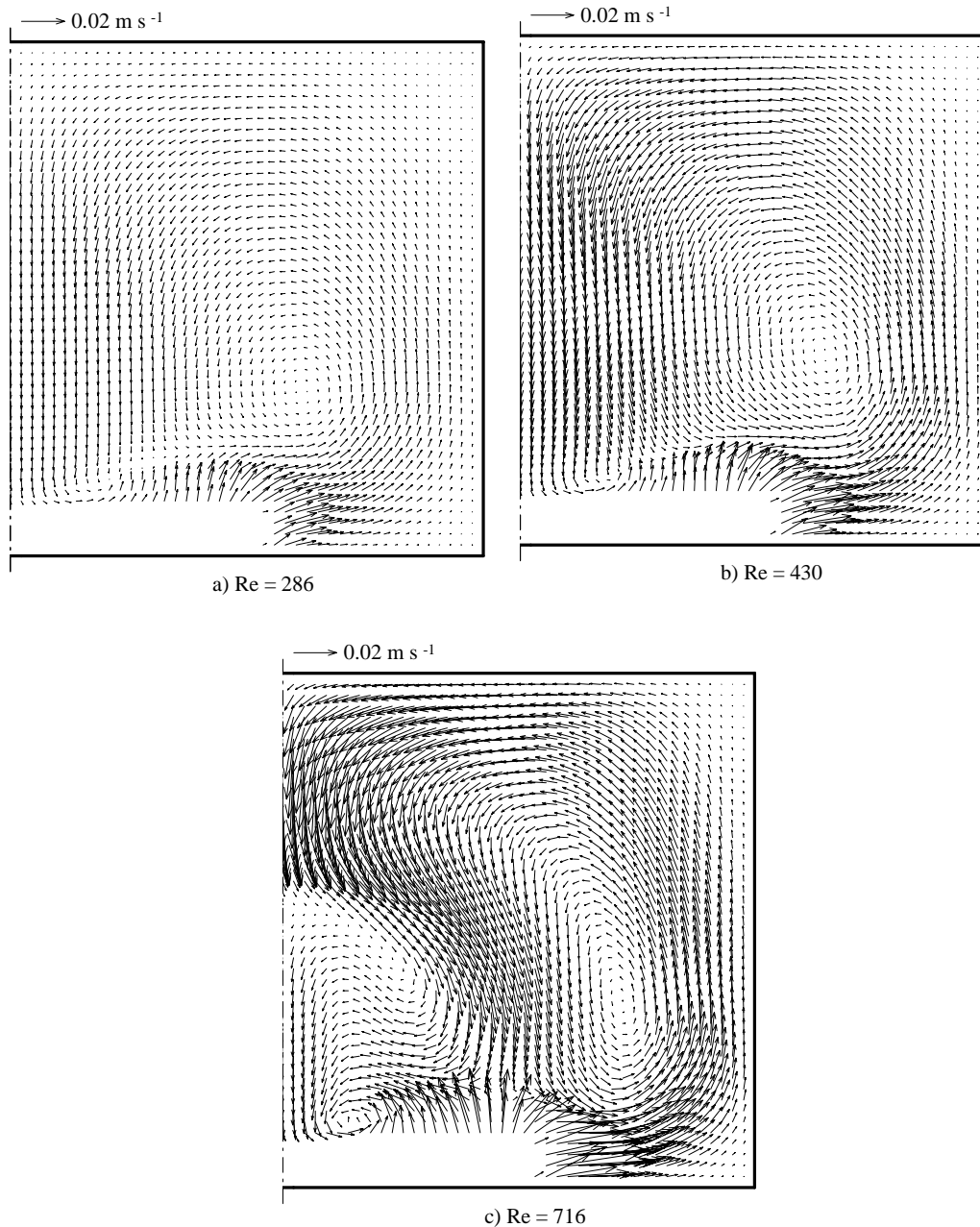


**Figure 4** : Velocity field in a vertical plane at angular coordinate from rod  $\theta = 0^\circ$  ; a)  $Re = 286$ , b)  $Re = 430$ ; c)  $Re = 716$ .

At high  $Re$  of 716 (Fig 4c), the vortices generated by the rotating rod are different from those at smaller Reynolds numbers. There is a well defined vortex breakdown near the axial region, which is similar to that of the swirling flow in a cylindrical container (Escudier, 1984; Lopez, 1990). In the present flow situation, the critical Reynolds number for vortex breakdown was found to be about 580. The recirculation flow, though beneficial for enhancing

medium mixing, may be detrimental to cell culture as it may have the effect of centrifuging cells towards the micro-bioreactor wall.

### 3.2 Medium Mixing

From the velocity distribution (Fig. 4), the flow in the upper part of the chamber is weak. The mixing in this region may be poor because the axial mass-transfer is

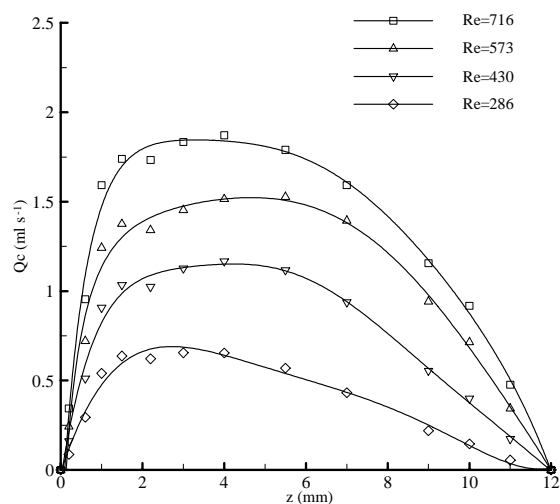


**Figure 5 :** Variation of circulation capacity with height at various Reynolds number.

largely dependent on axial velocity components, as generated by the secondary circulation. The circulation capacity (Costes and Couderc, 1988; Kunciewicz, 1992; Dong et al., 1994) is defined as:

$$Qc = \frac{1}{2} \int_A |V_z| dA \quad (8)$$

where  $|V_z|$  is the modulus of axial velocity component  $V_z$ , and  $dA$  is the incremental area over which  $V_z$  acts. Since a mass balance shows that the upward and downward flows are equal at any horizontal plane, the circulation capacity  $Qc$  is therefore the upward axial-flow rate through a certain horizontal plane. A larger axial upward flow rate will give better mixing. The circulation capacity along the vertical direction at different Reynolds numbers is presented in Fig 5. For each Reynolds number, the circulation capacity  $Qc$  reaches a maximum at height of  $z = 2$  mm plane that is just above the rod. Then it decreases gradually with height. At higher Reynolds number, the circulation capacity is larger, giving enhanced mixing.

The dimensionless form of the circulation capacity is the circulation coefficient:

$$N_{Qc} = \frac{Qc}{ND^3} \quad (9)$$

Fig 6 shows the circulation coefficient along the height  $z$  at different Reynolds numbers. The trends of the circulation coefficient  $N_{Qc}$  at different Reynolds numbers are

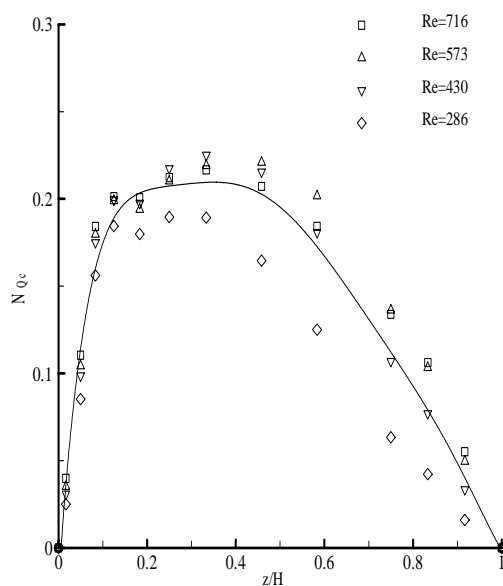


**Figure 6 :** Variation of circulation coefficient with height at various Reynolds numbers.

rather similar and so are their magnitudes, indicating an approximate collapse of data. Therefore the circulation coefficient  $N_{Qc}$  may be considered a non-dimensional parameter independent of Reynolds number. The maximum circulation coefficient is about 0.21 and occurs at a height  $z$  of 2 mm.

The circulation coefficient of the present stirred-rod is small compared with that of impellers in larger bioreactors, for which the circulation coefficient is around 1.0 in a one-litre bioreactor (Dong et al., 1994). One reason for the difference is that their impeller has six blades but the present magnetic rod is equivalent to only two blades. Furthermore the diameter of the present rod is small and its profile is not aerodynamically designed. Also, the present stirring rod is located at the bottom of the chamber, which is not effective for flow mixing. The small circulation coefficient indicates that fluid mixing is not high in the present micro-bioreactor. Thus it is necessary to check whether mass transport is adequate, particularly for oxygen transfer without bubble aeration.

### 3.3 Oxygen transfer

The oxygen-concentration distributions in the micro-bioreactor at various Reynolds and Damkholer numbers are presented in Figs 7a and 7b. The oxygen concentration level is non-dimensionalized by its saturation-concentration in the medium. The oxygen concentration

is low in the central region above the stirrer-rod tip (Fig 7a) because of the low mass-transport in the recirculation region there (Fig 4a). The Reynolds number of 286 is too low to provide sufficient mixing, thus the oxygen concentration is not high. At a higher Reynolds number of 716 (Fig 7b) the concentration distribution is more uniform than that at the lower Reynolds number. The concentration is still low in the region above the stirrer-rod tip because of the recirculation region there (Fig 4c). The concentration is higher in the region of the vortex-breakdown bubble (Fig 4c) due to higher flow-velocities there which convect oxygen from the top surface.

From the oxygen concentration field, its minimum values were determined and are presented in Fig. 8 at various Reynolds and Damkohler numbers. The minimum concentration is lower at smaller Re due to poor mixing as expected; and it is also lower at higher Damkohler number due to higher consumption by the cells.

The critical value of the dimensionless oxygen-concentration that causes cell hypoxia for CHO is 0.05 (Lin and Miller, 1992). Assuming the Damkohler number of CHO is less than 50, operating the micro-bioreactor at the small rotating speed corresponding to Re 286 (Fig 8) would be adequate to achieve sufficient oxygen transfer. The critical oxygen concentration of rat hepatocytes is 0.035 (Roy et al., 2001). However its Damkohler number is above 50, which thus requires a higher operating speed with Reynolds number above 286. When operating at rod Reynolds number of 716, the micro-bioreactor can support animal cell culture up to Damkohler number of 120 (Fig 8), assuming a critical value of 0.05 for the dimensionless oxygen-concentration.

From the oxygen concentration-field, the volumetric oxygen-transfer coefficient is determined from:

$$OTR = k_L a (C_0 - C_m) \quad (10)$$

where  $OTR$  is the volumetric oxygen-transfer rate,  $k_L a$  is the volumetric oxygen-transfer coefficient,  $C_0$  is the oxygen saturation-concentration in the medium, and  $C_m$  is the average oxygen-concentration. The average oxygen-concentration  $C_m$  may be determined from the concentration field. At steady state, the oxygen transferred into the micro-bioreactor is in equilibrium with the oxygen consumed by the cells. Thus the volumetric oxygen-transfer rate  $OTR$  may be calculated from volumetric integration of Eq. 5 using the oxygen concentration-field.

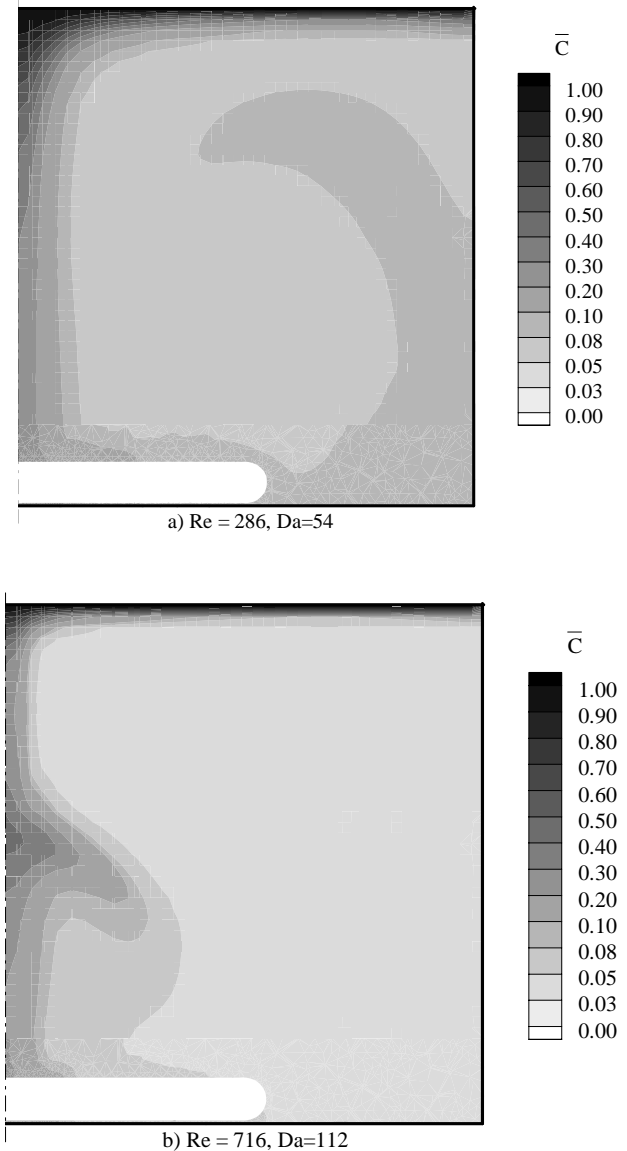


**Figure 7 :** Oxygen-concentration field in a vertical plane at angular coordinate from rod  $\theta = 0^\circ$ ; a) Re = 286, Da = 54; b) Re = 716, Da = 122.

The oxygen-transfer coefficient is an important parameter in the performance of bioreactors. The transfer coefficient is useful for determining the oxygen transfer in a bioreactor, for laboratory-scale use or when scaling up to a larger process. The coefficient has been used to measure the oxygen-uptake rate of cells, that is an important experimental parameter to monitor and control cell culture experiments (Ruffieux et al., 1998; Oliveira et al., 2005).

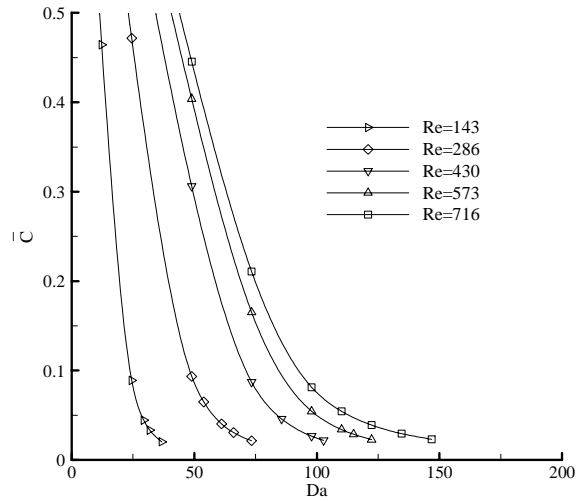


**Figure 8** : Minimum oxygen-concentration against Damkohler number at various Reynolds number.

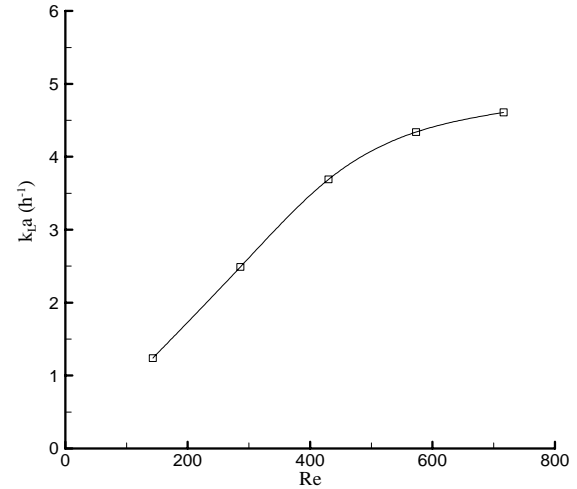


**Figure 9** : Variation of volumetric oxygen-transfer coefficient with Reynolds number.

The oxygen transfer coefficient  $k_L a$  of the micro-bioreactor operating at various Reynolds numbers is presented in Fig 9. The result is not affected by Damkohler numbers, within a reasonable range, because the oxygen transfer coefficient is a characteristic of the stirring system and does not depend on the cell consumption rate.

For the present range of Reynolds number (Fig 9), the oxygen-transfer coefficient  $k_L a$  is less than  $5 \text{ h}^{-1}$ . It is small compared with the  $k_L a$  of  $16.8 \text{ h}^{-1}$  in a two-litre centrifugal-impeller bioreactor with aeration sparger (Zhong et al, 2002); indeed their study determined that the plant cell growth was limited when the oxygen transfer coefficient was lower than  $6.4 \text{ h}^{-1}$ . In the case of bacteria culture, an oxygen transfer coefficient  $k_L a$  of up to  $768 \text{ h}^{-1}$  has been achieved in a 10-litre fermentor with aeration (Badino et al, 2001).

The present micro-bioreactor would be unable to generate sufficient oxygen transfer for bacteria and plant culture. Clearly for bacteria culture, aeration is needed to achieve adequate oxygen transfer as was used by Kostov et al. (2001). However for animal cell cultures which have a lower oxygen uptake rate, the critical oxygen-concentration level in the present micro-bioreactor, as shown earlier for CHO cells and hepatocytes, is adequate without using aeration bubbles which may cause cell trauma (Wang et al., 1994).

### 3.4 Hydrodynamic Stress

Animal cells are sensitive to hydrodynamic stress (Chisti, 2001) and its effects have been studied (see for example Schurch et al., 1988, Zhang et al., 1995). In this section, results of shear stress, normal stress and energy dissipation rate will be presented.

The three shear stress components in cylindrical coordinates (Currie, 2002) are:

$$S_{r\theta} = \mu \left[ r \frac{\partial}{\partial r} \left( \frac{V_\theta}{r} \right) + \frac{1}{r} \frac{\partial V_r}{\partial \theta} \right] \quad (11)$$

$$S_{\theta z} = \mu \left[ \frac{\partial V_\theta}{\partial z} + \frac{1}{r} \frac{\partial V_z}{\partial \theta} \right] \quad (12)$$

$$S_{rz} = \mu \left[ \frac{\partial V_z}{\partial r} + \frac{\partial V_r}{\partial z} \right] \quad (13)$$

The mean shear-stress level is defined from the resultant stress (Begley and Kleis, 2000):

$$S_M = \frac{1}{3} (S_{r\theta}^2 + S_{\theta z}^2 + S_{rz}^2)^{\frac{1}{2}} \quad (14)$$

The mean shear-stress levels are shown in Fig 10. Their values are relatively low inside throughout the micro-bioreactor. The maxima of mean shear-stresses are found to occur near the rod and its wake region; and the peak value is near the tip of the rod (see Fig. 10).

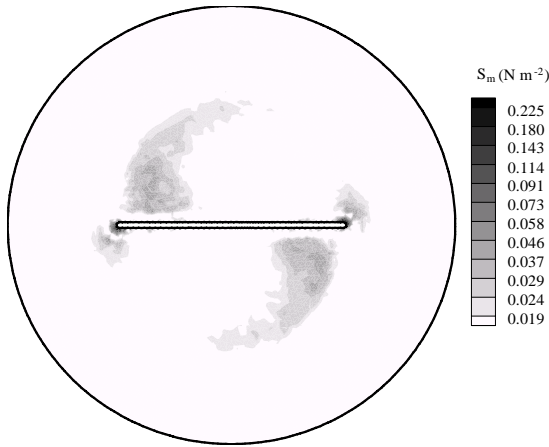


**Figure 10** : Shear-stress field in a horizontal plane at  $z/H = 0.01$  and Reynolds number  $Re = 430$ .

The peak shear stress at different Reynolds numbers is presented in Fig 11 (that also shows the normal stress to be discussed later). The peak shear-stress is below  $0.5 \text{ N m}^{-2}$ , that is not large. The present shear-stress is comparable to the experimental value of  $0.26 \text{ N m}^{-2}$  for the shear stress in a stirred bioreactor obtained by Joshi et al., (1996).

Mammalian cells are sensitive to high shear stress which may affect their viability and functions, and may even damage them. For hybridoma cell line, Born et al. (1992) reported that laminar shear stress up to  $208 \text{ N m}^{-2}$ , acting for 20 minutes, in un aerated flow led to substantial loss in cell count and viability. For CHO-K1 cells, Shiragami and Unno (1994) found that shear stress of  $0.7 \text{ N m}^{-2}$  caused cell detachment from the surface. Thus the peak shear-stress of below  $0.5 \text{ N m}^{-2}$  in the present micro-bioreactor is acceptable for animal cell culture.

Besides the shear stress, also of detriment to cells are the normal stress as found by Joshi et al.( 2001); Garcia-Briones and Chalmers (1994). In a stirred tank bioreactor, the normal stress would be of the same order of magnitude as the shear stress. The three normal stress components in cylindrical coordinates (Currie, 2002) are:

$$S_{rr} = 2\mu \frac{\partial V_r}{\partial r} \quad (15)$$

$$S_{\theta\theta} = 2\mu \left[ \frac{V_r}{r} + \frac{1}{r} \frac{\partial V_\theta}{\partial \theta} \right] \quad (16)$$

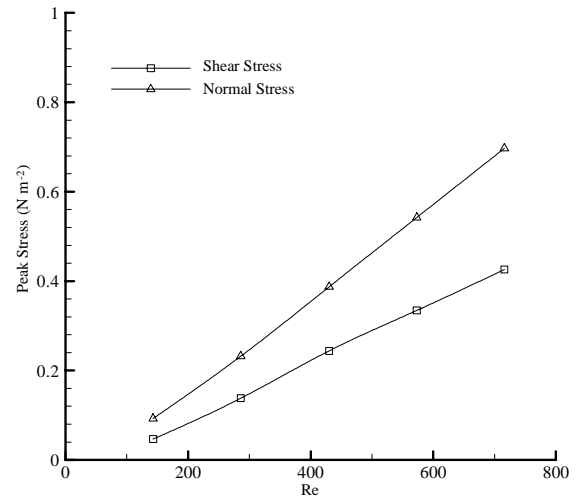


**Figure 11** : Peak values of shear and normal stresses against Reynolds number.

$$S_{zz} = 2\mu \frac{\partial V_z}{\partial z} \quad (17)$$

The mean normal stress may be defined as:

$$S_N = \frac{1}{3} (S_{rr}^2 + S_{\theta\theta}^2 + S_{zz}^2)^{\frac{1}{2}} \quad (18)$$

The normal stress-field has a rather similar distribution and magnitude as the shear stress. The values of mean normal stress are relatively low throughout the micro-bioreactor, with high values near the rod and its wake region. The peak normal stress at various Reynolds number is presented in Fig 11. At the same Reynolds number, the peak normal stress is about twice the peak shear stress.

It has been proposed that the damaging hydrodynamic forces on cells arise from the velocity gradients. Hence, the energy dissipation rate, that includes all velocity gradient components, may be used to evaluate the hydrodynamic environment. The energy dissipation levels in bioreactors have been related to cell damage (Garcia-Briones and Chalmers, 1994; Gregoriade et al., 2000; Ma et al., 2002). The energy dissipation rate is expressed as:

$$\Phi = \mu [(\nabla \vec{u} + \nabla \vec{u}^T) : \nabla \vec{u}] \quad (19)$$

Fig 12 shows the distribution of local energy dissipation rate in the micro-bioreactor. The maximum value

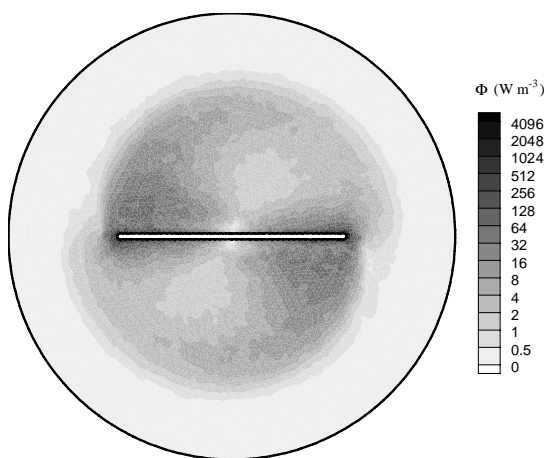


**Figure 12** : Distribution of local energy dissipation-rate in a horizontal plane  $z/H = 0.01$  at  $Re = 430$ .

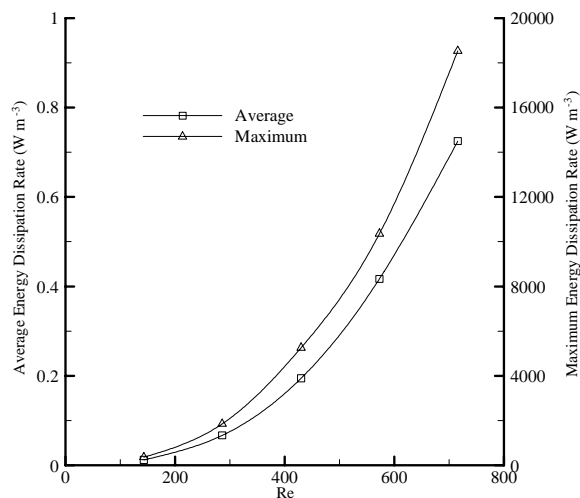


**Figure 13** : Average and maximum values of energy dissipation rate at various Reynolds number.

lies near the tip of the rod. The maximum and volume-averaged values of energy dissipation rate are presented in Fig 13. The maximum local energy dissipation rate is below  $18,000 W m^{-3}$ . In comparison a value of  $90,000 W m^{-3}$  was determined in a 10 litre vessel equipped with one Rushton impeller (Zhou and Kresta, 1996). The maximum energy dissipation rate in the present micro-bioreactor is acceptable as it is much smaller than the damaging value for CHO cell line, which is in the range of  $10^4 kW m^{-3}$  (Gregoriade et al., 2000).

It is noted that the ratio of maximum to mean values of the energy dissipation rate is in the order of four (Fig 13). For other bioreactors, the ratio is of order two (Zhou and Kresta, 1996; Ma et al., 2002). The present high-ratio is attributed to the stirrer being located at the bottom of the micro-bioreactor, that generates higher velocity gradients and hence high energy dissipation rate.

#### 4 Concluding remarks

A numerical model was developed for a micro-bioreactor, of working volume below 5 ml, in which the medium was mixed by a magnetic stirrer rod at the base. The fluid mixing, oxygen concentration and hydrodynamic stresses in the micro-bioreactor were evaluated with a view to applications in animal cell culture.

The computed flow field shows that a recirculation re-

gion arises above the rotating stirrer-rod, that provides the medium mixing in the axial direction. The medium mixing is characterized by a circulation coefficient of about 0.2, which is about 5 times smaller than that in a one-litre bioreactor with six impellers. Thus a high rotational speed is needed to ensure adequate mixing, as indicated by the results of the concentration-level and transfer-coefficient of oxygen.

At the highest rotation speed studied, rod Reynolds number of 716, the volumetric oxygen-transfer coefficient of the micro-bioreactor is around  $5 h^{-1}$  that is small compared with the value of  $768 h^{-1}$  achieved in a 10-litre bacteria-culture bioreactor with aeration. Thus for bacteria culture, it is necessary to enhance oxygen transfer by bubble aeration as was used by Kostov et al. (2001). However, the oxygen-concentration level in the present micro-bioreactor is adequate for certain animal-cell cultures without using bubble aeration. Assuming a critical value of 0.05 for the dimensionless oxygen-concentration, animal cell with Damkholer number up to 120 may be grown in the micro-bioreactor if operated at a high Reynolds number of 716.

The peak shear stress, at the high Reynolds number of 716, is around 0.5 Pa which is around two times that in a large scale stirred-tank bioreactor but, nevertheless, still below the level acceptable for animal cell culture. The maximum energy dissipation rate (that characterizes

the detrimental velocity gradients) is  $18 \text{ kWm}^{-3}$ ; that is around 5 times lower than that in a 10 litre stirred-tank bioreactor fitted with a Rushton impeller. Hence the hydrodynamic stress environment would be acceptable for animal cell culture when the micro-bioreactor is operated at the high Reynolds number of 716.

## References

- Badino Jr.; A.C.; Facciotti, M. C. R.; Schmidell, W.** (2001): Volumetric oxygen transfer coefficients ( $k_L a$ ) in batch cultivations involving non-Newtonian broths, *Biochem. Eng. J.* 8, 111–119.
- Batchelor, G. K.** (1967): *An introduction to fluid dynamics*. Cambridge. Cambridge University Press.
- Begley, C. M.; Kleis, S. J.** (2000): The fluid dynamic and shear environment in the NASA/JSC rotating-wall perfused-vessel bioreactor. *Biotechnol. Bioeng.* 70, 32–40.
- Born, C.; Zhang, Z.; Al-Rubeai, M.; and Thomas, C. R.** (1992): Estimation of disruption of animal cells by laminar shear stress. *Biotechnol. Bioeng.* 40, 1004–1010.
- Chisti, Y.** (2001): Hydrodynamic damage to animal cells. *Crit. Rev. Biotechnol.* 21, 67–110.
- Costes, J.; Couderc, J. P.** (1988): Study by laser Doppler anemometry of the turbulent flow induced by a Rushton turbine in a stirred tank: Influence of the size of the units - I. Mean flow and turbulence. *Chem. Eng. Sci.* 43, 2751–2772.
- Currie, I. G.** (2002): *Fundamental mechanics of fluids*. New York: Marcel Dekker.
- Deshpande, R. R.; Heinze, E.** (2004): On-line oxygen uptake rate and culture viability measurement of animal cell culture using microplates with integrated oxygen sensors. *Biotechnol. Lett.* 26, 763–767.
- Dong, L.; Johansen, S. T.; Engh, T. A.** (1994): Flow induced by an impeller in an unbaffled tank - I. *Experimental. Chem. Eng. Sci.* 49, 549–560.
- Escudier, M. P.** (1984): Observations of the flow produced in a cylindrical container by a rotating wall, *Exp. Fluids.* 2, 189–196.
- Garcia-Briones, M. A.; Chalmers, J. J.** (1994): Flow parameters associated with hydrodynamic cell injury. *Biotechnol. Bioeng.* 44, 1089–1098.
- Girard, P.; Jordan, M.; Tsao, M.; Wurm, F. M.** (2001): Small-scale bioreactor system for process development and optimization. *Biochem. Eng. J.* 7, 117–119.
- Gregoriades, N.; Clay, J.; Ma, N.; Koelling, K.; Chalmers, J. J.** (2000): Cell damage of microcarrier cultures as a function of local energy dissipation created by a rapid extensional flow. *Biotechnol. Bioeng.* 69, 171–182.
- Harvey, A. D.; West, D. H.; Tuffillaro, N. B.** (2000): Evaluation of laminar mixing in stirred tank using a discrete-time particle mapping procedure. *Chem. Eng. Sci.* 55, 667–684.
- Joshi, J. B.; Elias, C. B.; Patole, M. S.** (1996): Role of hydrodynamic shear in the cultivation of animal, plant and microbial cells. *Chem. Eng. Sci.* 62, 121–141.
- Joshi, J. B.; Sawant, S. B.; Patwardhan, A. W.; Patil, D. J.; Kshatriya, S. S.; Nere, N. K.** (2001): Relation between flow pattern and de-activation of enzymes in stirred reactors. *Chem. Eng. Sci.* 56, 443–452.
- Kostov, Y.; Harms, P.; Randers-Eichhorn, L.; Rao, G.** (2001): Low-cost micro-bioreactor for high-throughput bioprocessing. *Biotechnol. Bioeng.* 72, 346–352.
- Kumar, S.; Wittmann C.; and Heinze E.** (2004): Minibioreactors. *Biotechnol. Lett.* 26, 1–10.
- Kuncewicz, C.** (1992): Three-dimensional model of laminar liquid flow for paddle impellers and flat-blade turbines. *Chem. Eng. Sci.* 47, 3959–3967.
- Lappa, M.** (2003): Organic tissues in rotating bioreactors: Fluid-mechanical aspects, dynamic growth models, and morphological evolution. *Biotech. Bioeng.* 84, 518–532.
- Leist, C. H.; Meyer, H. -P.; Fiechter, A.** (1990): Potential and problems of animal cells in suspension culture. *J. Biotech.* 15, 1–46.
- Lin, A. A.; Miller, W. M.** (1992): CHO cell responses to low oxygen: regulation of oxygen consumption and sensitization to oxidative stress. *Biotechnol. Bioeng.* 40, 505–516.
- Lopez, J. M.** (1990): Axisymmetric vortex breakdown Part 1 - Confined swirling flow. *J. Fluid Mech.* 221, 533–552.
- Lubbert, A.; Jorgensen, S. B.** (2001): Bioreactor performance: a more scientific approach for practice. *J. Biotech.* 85, 187–212.
- Ma, N.; Koelling, K. W.; Chalmers, J. J.** (2002): Fabrication and use of transient contractional flow device to quantify the sensitivity of mammalian and insect cells to hydrodynamic forces. *Biotechnol. Bioeng.* 80, 428–437.

- Nagata, S.** (1975): *Mixing – Principles and Applications*. New York: Wiley, p 458.
- Ng, K.; Borrett, N. A.; Yianneskis, M.** (1999): On the distribution of turbulence energy dissipation in stirred vessels. *I ChemE Symp. Series*. 146, 69-80.
- Oliveira, R.; Clemente, J. J.; Cunha, A. E.; Carrondo, M. J. T.** (2005): Adaptive dissolved oxygen control through the glycerol feeding in a recombinant *Pichia pastoris* cultivation in conditions of oxygen transfer limitation. *J. Biotechnol.* 116, 35-50.
- Roy, P.; Baskaran, H.; Tilles, A. W.; Yarmush, M. L.; Toner, M.** (2001): Analysis of oxygen transport to hepatocytes in a flat-bed microchannel bioreactor, *Ann. Biomed. Eng.* 29, 947-955.
- Ruffieux, P.-A.; von Stockar, U.; Marison, I. W.** (1998): Measurement of volumetric (OUR) and determination of specific ( $qO_2$ ) oxygen uptake rates in animal cell cultures. *J. Biotechnol.* 63, 85-95.
- Schurch, U.; Kramer, H.; Einsele, A.; Widmer, F.; Eppenberger, H. M.** (1988): Experimental evaluation of laminar shear-stress on the behavior of hybridoma mass cell-cultures, producing monoclonal-antibodies against mitochondrial creatine-kinase. *J. Biotechnol.* 7, 179-184.
- Shiragami, N.; Unno, H.** (1994): Effect of shear stress on activity of cellular enzyme in animal cell. *Bioprocess Eng.* 10, 43-45.
- Unger, D. R.; Muzzio, F. J.; Auninsm J. G.; Singhvi, R.** (2000): Computational and experimental investigation of flow and fluid mixing in the roller bottle bioreactor. *Biotech. Bioeng.* 70, 117-130.
- Venkat, R. V.; Stock, L. R.; Chalmers, J. J.** (1996): Study of hydrodynamics in microcarrier culture spinner vessels: a particle tracking velocimetry approach. *Biotech. Bioeng.* 49, 456-466.
- Wang, N. S.; Yang, J. D.; Calabrese, R. V.; Chang, K. C.** (1994): Unified modeling framework of cell death due to bubbles in agitated and sparged bioreactors. *Biotechnol.* 33, 107-122.
- Williams, K. A.; Saini, S.; Wick, T. M.** (2002): Computational fluid dynamics modeling of steady-state momentum and mass transport in a bioreactor for cartilage tissue engineering. *Biotechnol. Prog.* 18, 951-963.
- Youcefi, A.** (1993): *Etude expérimentale de l'Écoulement d'un Fluide Viscoélastique Autour d'un Agitateur Bipale en cuve agitée*. Thèse de Doctorat. INP Toulouse, France.
- Zalc, J. M.; Alvarez, M. M.; Muzzio, F. J.; Arik, B. E.** (2001): Extensive validation of computed laminar flow in a stirred tank with three Rushton turbines. *AIChE J.* 47, 2144-2154.
- Zhang, Z.; Chisti, Y.; Moo-Young, M.** (1995): Effects of the hydrodynamic environment and shear protectants on survival of erythrocytes in suspension. *J. Biotechnol.* 43, 33-40.
- Zhong, J. J.; Pan, Z. W.; Wang, Z. Y.; Wu, J. Y.; Chen, F.; Takaji, M.; Yoshida, T.** (2002): Effect of mixing time on taxoid production using suspension cultures of *Taxus chinensis* in a centrifugal impeller bioreactor. *J. of Biosci. Bioeng.* 94, 244-250.
- Zhou, G.; Kresta, S. M.** (1996): Impact of tank geometry on the maximum turbulence energy dissipation rate for impellers. *AIChE J.* 42, 2476-2490.